A LIGHTNING PREDICTION INDEX THAT UTILIZES GPS INTEGRATED PRECIPITABLE WATER VAPOR

by

Robert A. Mazany[1], Steven Businger[2], Seth I. Gutman[3], and William Roeder[4]

submitted to Weather and Forecasting

Revised February 2001

[1] University of Hawaii, Honolulu, HI (Current affiliation: 17th Operational Weather Squadron, Joint Typhoon Warning Center, Pearl Harbor, Hawaii 96829)

[2] Corresponding Author: Department of Meteorology, University of Hawaii, 2525 Correa Rd., Honolulu, HI, 96822

[3] NOAA Forecast Systems Laboratory R/FS3, Boulder, CO 80305

[4] Patrick Air Force Base, FL 32925

ABSTRACT

The primary weather challenge at the Cape Canaveral Air Station and Kennedy Space Center is lightning. In this paper we describe a statistical approach that combines integrated precipitable water vapor (IPWV) data from a global positioning system (GPS) receiver site located at the Kennedy Space Center with other meteorological data to develop a new *GPS lightning index*. The goal of this effort is to increase the forecasting skill and lead time of a *first strike* at Cape Canaveral and the Kennedy Space Center. Statistical regression methods are used to identify predictors that contribute skill in forecasting a lightning event. Four predictors were identified out of a field of 23 predictors that were tested, determined using data from the 1999 summer thunderstorm season. They are maximum electric field mill values, GPS IPWV, nine-hour change in IPWV, and K index. The *GPS lightning index* is a binary logistic regression model comprised of coefficients multiplying the four predictors.

When time series of the GPS lightning index are plotted, a common pattern emerges several hours prior to a lightning event. Whenever the GPS lightning index falls to 0.7 or below, lightning occurs within the next 12.5 hours. An index threshold value of 0.7 was determined from the data for lightning prediction. Forecasting time constraints based on the Kennedy Space Center (KSC) criteria were incorporated into the verification. Forecast verification results obtained by using a contingency table revealed a 26.2% decrease from the Cape's previous season false alarm rates for a non-independent period and a 13.2% decrease in false alarm rates for an independent test season using the GPS lightning index. Additionally, the index improved the KSC desired lead time by nearly 10%. Although the lightning strike window of 12 hours is long, the GPS lightning index provides useful guidance to the forecaster in preparing lighting forecasts, when combined with other resources such as radar and satellite data. Future testing of the GPS lightning index and the

prospect of using the logistic regression approach in forecasting related weather hazards are discussed.

1. Introduction

Space launches and landings at the Cape Canaveral Air Station (CCAS) and the Kennedy Space Center (KSC) are subject to strict weather–related constraints (e.g., Bauman and Businger 1996). Nearly 75% of all space shuttle countdowns between 1981 and 1994 were delayed or scrubbed, with about half of these due to weather (Hazen et al. 1995). Of the various weather constraints, the primary weather challenge is to forecast lightning 90 minutes before a *first strike* and within a 20-nm radius of the complex. The National Lightning Detection Network indicates that this region has the highest lightning flash density in the country, averaging 10 flashes/km^2/yr, confirming that lightning has a significant impact on the Kennedy Space Center. The first concern is the safety of personnel working on the complex, and the next is protection for $10 billion rocket launching systems and platforms that include the Space Shuttle, Athena, Pegasus, Atlas, Trident II, and Titan IV. Finally, delay costs can run anywhere from $90,000 for a 24-hour delay to $1,000,000 if the Shuttle must land at another facility and be transported back to the KSC.

Modeling and observational studies conclude that patterns and locations of Florida convection are related to the interaction of the synoptic wind field with the mesoscale sea-breeze (Estoque 1962; Neumann 1971; Pielke 1974; Boybeyi and Raman 1992). The sea-breeze circulation and patterns of convection have different characteristics dependent on whether or not the low-level flow has onshore, offshore, or an alongshore component with respect to Florida's east coast (Aritt 1993).

Onshore easterly flow typically generates less vigorous convection than offshore westerly flow (Foote 1991). However, onshore flow is characterized by a shallow low-level maritime moist layer, capped by a subsidence layer with dry conditions aloft, creating difficulties in predicting convection associated with this type of regime (Pielke 1974; Bauman et al. 1997). Blanchard and Lopez (1985) show that the majority of convection takes place in the sea-breeze and lake-breeze convergence zones. They state that deep convection is sparse and requires low-level forcing which generally occurs only when the east coast sea-breeze has advanced westward and merges with the west coast sea-breeze. Although convection can develop independently of a sea-breeze frontal merge, it is usually weaker than when the fronts merge.

Reap (1994) found that southwesterly flow tends to be more unstable and produce more lightning strikes along the Florida east coast than easterly flow. The southwesterly flow also contains deeper moisture and accounts for two-thirds of the lightning strikes during the summer at KSC. In contrast, easterly flow only accounts for less than 5% of the total lighting flashes (Watson et al. 1991).

The International Station Meteorological Climate Summary for Cape Canaveral (Mar 68- Feb 78) indicates an annual average of 76 days with thunderstorms. Most of the thunderstorms (81.2%) occur from May through the end of September. In fact, the 45th Weather Squadron (WS) at Patrick Air Force Base can issue more than 1200 lightning watches and warning per year.

The 45th WS uses numerical weather prediction models and many observation systems to detect and predict lightning in support of the space center needs. The latter include satellite data, weather radars, rawinsondes, and five lightning detection systems. The lightning detection and ranging (LDAR) is a seven-antenna radio-wave time-of-arrival system that provides a three-dimensional picture of in-cloud, cloud-to-cloud, cloud-to-clear air, and cloud-to-ground lightning.

The Cloud to Ground Lightning Surveillance System is a 5-antenna magnetic direction finding system. The launch pad lightning warning system (LPLWS) is a network of 31 surface electric field mills. The national lightning detection network (NLDN) is a national network of magnetic direction finding and time-of-arrival antennas. The A.D. Little Corp sensor is an older system using one antenna to estimate the lightning distance from the magnetic pulse change. Most of these lighting detection systems are more fully described by Harms et al. (1997).

For the 1999 thunderstorm season, the 45th WS capability to detect thunderstorms is 97.5%, 79.1% of which meet the desired lead-time. The KSC false alarm rate is 43.2%. There is room for improvement in these statistics, particularly in reducing the false alarm rate.

GPS and the Role of Water Vapor

Water plays a critical role in a variety of atmospheric processes that act over a wide range of temporal and spatial scales. It is the most variable of the major constituents of the atmosphere. The distribution of water vapor is closely coupled with the distribution of clouds and rainfall. Because of the large latent heat release of water vapor during a phase change, the distribution of water vapor plays a crucial role in the vertical stability of the atmosphere and evolution of storm systems.

The water molecule has a unique structure that results in a permanent dipole moment that is caused by an asymmetric distribution of charge in the water molecule. Several different mechanisms have been proposed to account for generation of electrical charge separation in clouds. However, only the polarization mechanism has been shown by numerical modeling to be capable of generating the amounts of charge at rates typical of thunderstorms (e.g., Fleagle and Businger 1980, p. 139). When collisions occur between the falling grauple and a cloud droplet or ice pellet,

a negative charge is transferred to the grauple, leaving the droplet or ice pellet positively charged. The smaller particle, now with positive charge, is carried upward in the updrafts, while the heavier grauple carries the negative charge downward. This process is reinforcing because as charges are separated, the electric field strength increases, thus increasing both polarization and the transfer of charge occurring at each collision.

Bevis et al. (1992, 1994) describe the methodology for using GPS to monitor atmospheric water vapor from ground-based GPS sites and explore the error analysis of GPS precipitable water. Duan et al. (1996) provide the first direct estimation of integrated precipitable water (IPWV) by eliminating any need for external comparison with water vapor radiometer observations. Businger et al. (1996) describe meteorological applications of atmospheric monitoring by GPS for use in weather and climate studies and in numerical weather prediction models.

The National Oceanic and Atmospheric Administration (NOAA) Forecast Systems Laboratory established the first GPS network dedicated to atmospheric remote sensing of water vapor (Wolfe and Gutman 2000). Since its inception in 1994, the NOAA GPS network has been steadily expanding, with GPS receivers sited or planned in all 50 states. Florida, like many other states, has plans to develop a relatively large network of GPS receivers for applications other than weather forecasting (Fig. 1). The dual use of these sites, however, is expected to provide valuable data for the improvement of short-term cloud and precipitation forecasts, with consequent improvements in transportation safety. Recently, a sliding window technique for processing the GPS was developed jointly at UH and Scripps and implemented operationally at FSL that provides estimates of IPW every 30 minutes with about 18 minutes latency and an accuracy of ~3.5% (Fig. 2). GPS IPWV data are available in near real time on the web, courtesy of NOAA/FSL at http://gpsmet.fsl.noaa.gov/realtimeview/jsp/rti.jsp.

In this paper we describe a statistical approach that combines IPWV data from a GPS site located at the Kennedy Space Center with other meteorological data to develop a new *GPS lightning index*. The goal of this effort is to improve the skill in forecasting a *first strike* at Cape Canaveral and the Kennedy Space Center.

2. Data Resources

The thunderstorm season is from May through September. Data for the 1999 summer season were divided into two periods, a pre-season (14 April - 9 June 1999) and a thunderstorm season (10 June - 26 September 1999). These particular dates were chosen on the basis of the distribution of thunderstorms and the data availability associated with instrumentation down time.

The thunderstorm season data were used to create the logistic regression model that comprises the *GPS lightning index*. Thunderstorm season data contained 46 event days and provided robust predictor data. During this season, GPS IPWV values are much higher and show more variability than in the winter and preseason. The preseason data were reserved for an independent test using the GPS lightning index results.

Cape Canaveral has a dense array of weather sensors. One of the challenges of this research is determining which meteorological variables would add skill in a lightning prediction index. Twenty-three potential predictors were initially evaluated (Table 1). The availability of realtime GPS IPWV was the primary motivation for the undertaking the research presented in this paper. Since October 1998, GPS IPWV data have become available with 30-minute temporal resolution for a GPS site located at 28.48 N. latitude, 80.38 W longitude, roughly the center of the Cape just north of the primary landing strip. Data for this research cover one year from October 1998 to October 1999. The GPS site had missing data, mostly due to communications problems between

the site and the facility that collects the data for NOAA/FSL. Data from any day that contained partial data loss were eliminated from the analysis.

Cape Canaveral data resources offered benefits that make this study possible. Upper air soundings are often taken more than twice a day pending various launches and weather conditions, so there is a slight increase in the temporal resolution. Also, there are observers at the Cape 24 hours a day. Adding a human element to the observation codes, especially in the remarks section, provided an increase in understanding of the meteorological conditions. Electric field mills provided another source of data in this investigation. There are 31 field mills that measure the electric potential of the atmosphere in volts/meter (V/m) every five minutes. The maximum field mill value was used for the 30-minute window ranging from the top of the hour until the half-hour mark. This maximum value was assigned to the GPS IPWV value taken 15 minutes after the hour. From the half-hour mark to the top of the hour, that value was assigned with the GPS IPWV value taken 45 minutes after the hour. Typical fair weather electric field mill values ranged from 70 V/m to 800 V/m. During inclement weather when the potential for lightning existed, values would increase substantially, sometimes reaching values of 12,000 V/m during a lightning event. The only suspect values were around 1000 UTC (0500 EST). From a normal field of 100-200 V/m just before 1000 UTC, field mill values would jump, sometimes up to 3000 V/m for what appeared to be no meteorological event. Marshall et al. (1999) explain this *sunrise effect* as the local, upward mixing of the denser, low-lying, electrode-layer charge.

Other variables investigated for the GPS lightning index include 700-mb vertical velocity from the ETA model, total totals (TT) index, k-index (KI), freezing level from rawinsondes, and surface temperature, dewpoint, pressure, and wind direction taken from station observations. The KI considers the static stability of the 850-500-mb layer. The KI is given by the equation

$$KI = T_{850} - T_{500} + T_{d850} - (T_{700} - T_{d700}), \quad (1)$$

where T_{850} and T_{d850} are the dry bulb temperature and dewpoint at 850 mb, and T_{500} is the dry bulb temperature 500 mb. The quantity $T_{700} - T_{d700}$ is the 700-mb dewpoint depression. In order for the KI to correspond with the 30-minute GPS temporal resolution, KI values were interpolated linearly between sounding times.

Finally, Lightning Detection and Ranging (LDAR) data were used as *ground truth* to verify when and where a lightning event occurred. LDAR data are voluminous; the sensors detect step-leaders. With a time resolution on the order of milliseconds, one lightning flash can have up to 20,000 LDAR points, and one thunderstorm can have thousands of flashes, so one thunderstorm can have up to tens of millions of LDAR points. These LDAR points (in meters) are ranged from a central site in the *x*, *y*, and *z* directions. A point is classified as a new flash if the new point is 300 milliseconds (ms) later or 5000 meters from the previous point. Also, two or more points make a flash. This is same criterion that the National Weather Service, Melbourne FL, uses to actually verify step-leader points as a lightning flash. In the research presented in this paper, the first strike was verified using LDAR data and matched to the nearest corresponding GPS IPWV data.

3. Development of a Lightning Prediction Index

a. Logistic Regression

Regression methods provide the best opportunity for data analysis concerned with describing the relationship between a response variable and one or more predictor variables. Since the event to be forecast was the first strike of a lightning event, a binary logistic regression model was chosen as opposed to a linear regression model.

What distinguishes a logistic regression model from a linear regression model is that the outcome variable in logistic regression is binary or dichotomous (Hosmer and Lemeshow 1989). The two outcomes are *yes* the lightning event occurred or *no* it did not.

The quantity $\pi_j = E(Y|x_j)$ represents the conditional mean of a lightning strike (Y) given a predictor (x) when the logistic distribution is used. The specific form of the logistic regression model is

$$\pi_j = \frac{e^{(\beta_0 + \beta x_j)}}{1 + e^{(\beta_0 + \beta x_j)}}, \qquad (2)$$

where π_j is the probability of a response for the j^{th} covariate, β_0 is the intercept, β is a vector of unknown coefficients associated with the predictor, x_j is a predictor variable associated with the j^{th} covariate. Next, Hosmer and Lemeshow (1989) use a logit transformation of π_j defined as

$$g(\pi_j) = \ln [(\pi_j)/(1-\pi_j)] = \beta_0 + \beta_j X_j \qquad (3)$$

The importance of this link function is that $g(\pi_j)$ has many of the desirable properties of a linear model. The logit $g(x)$ is linear in its parameters, may be continuous, and may range from $-\infty$ to $+\infty$, depending on the range of x.

b. The Predictors

In order to determine what variables contribute significantly in the regression, the initial set of predictors included 23 in all (Table 1). In the table changes in IPWV with time (Δ-hr IPWV) for periods ranging from 1 to 12 hours are designated as variables 2 through 13. The purpose of including changes in IPWV is to capture differences in the air mass moisture over various periods of time. Positive values indicate that IPWV has increased over the time interval.

Logistic regression model output shows the estimates of the coefficients, standard error of the coefficients, z-values, p-values, and a 95% confidence interval for the odds ratio. Predictors that did not meet the 99% significance level, sometimes called the *p-value,* in the model results were eliminated.

Model output of the initial 23 variables left only four predictors that met the 99% significance level. These four are electric field mill maximum (V/m), GPS IPWV, Δ 9 hr IPWV, and KI. The coefficient of each predictor is the estimated change in the link function with a one-unit change in the predictor, assuming all other factors and covariates are the same. Given the fact that three of the variables are sensitive to moisture, it important to note that they are not well correlated. The highest correlation coefficient was 0.47 between IPWV and KI.

Statistical hypothesis testing is carried out by setting up a null hypothesis. If we set the coefficients to zero as the null hypothesis, the estimated coefficients in Table 2 show that the remaining predictors all have a p-value ≤ 0.01. This indicates that the parameters are not zero with a 99% significance level, and we can reject the null hypothesis and use our estimated coefficients. Further, review of the odds ratios in Table 2 indicates that some predictors have a greater impact than others. An odds ratio very close to one indicates that a one-unit increase minimally affects a lightning event. A more meaningful difference is found with Δ-9 hr IPWV. An odds ratio of 1.38 indicates that the odds of a lightning event increase by 1.38 times with each unit increase. The z-value is obtained by dividing the coefficient by its standard deviation. Dividing by the standard deviation weights the accuracy of the coefficient. Smaller standard deviations lead to larger z-values, positive or negative. Table 2 reflects the top four z-values and provides strong evidence that the coefficients are highly accurate and belong in the GPS lightning Index.

c. Relationship Between Predictors and Predictand

The relationship between time series of discrete events can be studied by a technique known as the s*uperposed epoch* method (Panofsky and Brier 1958). The *first strike* of lightning is defined as a discrete event since it is the critical component of the forecast for the Cape. Since lightning occurs at various times of the day, the superposed epoch method creates composites of the data surrounding the 27 lightning events during the thunderstorm period. For each lightning event the time of first strike was denoted as T_0. Hours prior to that key time were denoted as T_{0-1}, T_{0-2}, $T_{0-3,}$ etc. Figure 3a depicts the composite GPS IPWV values leading up to the first strike. The general increase in IPWV suggests a correlation between increasing IPWV values and the time of the first strike. Contrary to GPS IPWV, electric field mill values show random fluctuations leading right up to the first strike when the field mill values spike up to indicate a lightning event has occurred. In this case, there is very little warning time for forecasting lightning events. This predictor remains in the model because of its relationship with lightning 90 minutes prior to the first strike (Fig. 3a). Although this figure shows slight increases up until the first strike itself, in the 5-minute resolution (raw), the increases are much more dramatic.

Days containing no lightning at all, non-event days, have IPWV values that hover around 35 mm. The non-event graph depicts average GPS IPWV values for 20 days during the thunderstorm period (Fig. 3b). As seen in the graph, the 24-hr run is relatively flat, exhibiting minor fluctuations, including subtle nocturnal decline from 3:15 UTC (2200 EST) until 11:15 UTC (0600 EST) and a rise to 18:15 UTC (13:15 EST), that can be attributed to solar heating.

A series of scatter diagrams was used to document relationships between the predictors and the lightning events. The scatter plots show data for all thunderstorm days. Only the 30-minute data up to the time of the first lightning strike are plotted. No data following the first strike are

included in the plots. Lightning events were considered independent if there was a 12-hr period between the end of one lightning event and the of another. Figure 4a shows GPS IPWV values > 35 mm are more conducive for lightning strikes. Conversely, no first strike events were noted when the GPS IPWV values were < 33 mm.

When the KI is plotted with electric field mill data (Fig. 4b), a clear bias is present. Lightning events are much more likely to occur when the KI was $\geq$ 26. This stability index proved more relevant than the total totals index. A study on nowcasting convective activity for the KSC conducted by Bauman et al. (1997) concluded that of all the stability indices, only the KI was found to have a modest utility in discriminating convective activity. This can be attributed to the fact that the KI captures a moisture layer from 850mb to 700mb, as opposed to just one reference point of 850-mb dewpoint temperature by total totals. Typical Cape KI values ranging from 26-30 yield an air mass thunderstorm probability of 40-60%. A value of 31-35 yields a probability range of 60-80%, and 36-40 yields a probability of 80-90%. Values for this study hover around 50-60%, similar odds as flipping a coin.

Initially, changes of IPWV for one hour were used. Eventually, this was carried out to 12-hr IPWV changes. Again, the superposed epoch method was applied to the data. Use of the hourly Δ-1 to Δ-12 hourly IPWV predictors enabled the GPS lightning index to capture the IPWV changes of the air mass. As it turned out (statistically), the Δ9-hr IPWV predictor had more impact than the other ΔIPWV predictors. Looking at field mill values and Δ1-hr IPWV (Fig. 4c), lightning indicators values are scattered on either side of the zero line with the average value around 2.5 mm. When compared to the Δ9-hr IPWV plot (Fig. 4d), average Δ9-hr IPWV values are double the Δ1-hr averages and indicate no lightning strikes occurred below the zero line. Other intervals, such as Δ6 hr IPWV (not shown), do show a tendency of increased lightning as IPWV increased.

However, with the logistic regression model, the Δ9-hr IPWV prevails statistically as the best predictor. The Δ9-hr IPWV exhibits the most prominent increase of IPWV in the 5 hours prior to that first strike (Fig. 5).

The Δ9-hr IPWV predictor refers to a timeframe 9 hours prior to the first strike. Therefore, the Δ9-hr IPWV examines changes in IPWV on meteorological events that span the course of 9 hours. Figure 6 shows that most of the lightning events occur in mid to late afternoon. Mechanisms linked to this timeframe may include effects attributed to the diurnal cycle of solar heating and moisture properties associated with the sea breeze and, as discussed in the introduction, the impact of synoptic circulations.

The relationship between change in GPS IPWV and lightning occurrence proves a little more challenging to explain. Increases in the Δ9-hr IPWV indicate an increase in the amount of mid-level moisture that plays an important role in the stability of convective clouds. Moist air (as opposed to dry air) being entrained into these clouds will result in an increase in their buoyancy.

A possible mechanism for increased midlevel moisture is the interaction of various mesoscale boundaries associated with the geography in central Florida. A strong sea breeze from the western peninsula coast advances and interacts with the eastern coastal sea breeze. The Δ9-hr IPWV predictor could be detecting the increased moisture associated with sea breeze fronts. Other mechanisms include deeper moisture associated with southwesterly flow regimes, indicating an increase in the maritime moist layer (Reap 1994).

Another important mechanism is dynamics associated with the passage of jet streaks aloft (Bauman et al. 1997). Divergence aloft is associated with jet entrance and exit regions and draws moisture up to mid-levels in the troposphere.

4. Assessing the Utility of the GPS Lightning Index

To determine the effectiveness of the GPS lightning index in describing the outcome variable, the fit of the estimated logistic regression must now be assessed. This is referred to as goodness of fit. Hosmer and Lemeshow (1989) recommend three methods to determine goodness of fit; Pearson residual, deviance residual, and the Hosmer-Lemeshow test (Table 3). They also introduce a decile of risk method for observed and expected frequencies (Table 4) as well as measures of association between the response variable and the predicted probabilities (Table 5).

The p-values range from 0.605 to 1.000 for the Pearson and deviance residuals and for the Hosmer-Lemeshow tests (Table 3). This indicates that there is sufficient evidence for the model fitting the data adequately. If the p-values were less than the accepted level (0.05), the test would indicate sufficient evidence for a conclusion of an inadequate model fit.

The results of applying the decile of risk grouping strategy to the estimated probabilities computed from the model for lightning strikes are given in Table 4. The data in Table 4 are grouped by their estimated probabilities from lowest to highest in 0.1 increments. Thus, group 1 contains the data with the lowest estimated probabilities ($\leq$0.1) while group 10 contains data with the highest estimated probabilities (>0.9). Since the total number of lightning strikes is 995, each decile group total must be evenly distributed for proper comparison. Therefore, the Hosmer and Lemeshow strategy breaks down each group into a total of 99 or 100 events.

The following will help explain the meaning of Table 4. The observed frequency in the *yes* (y=0, a lightning strike) group for the seventh decile (<0.7) of risk is 26, meaning that there were 26 lightning events actually observed from the seventh decile group. These are the events that have an estimated probability of occurring of $\leq$0.7. In a similar fashion the corresponding estimated expected frequency for this seventh decile is 25.8, which is the sum of the modeled probabilities

for these lightning events to occur. The observed frequency for the *no* lightning (y=1) group is 99-26 = 73, and the estimated frequency is 99-25.8 = 73.2. Table 4 provides sufficient evidence that the model does fit the data well because the observed and expected frequencies are very close.

The values in Table 4 are calculated by pairing the observations with different response values. Here 221 *yes* lightning strikes and 774 *no* lightning events were recorded during the thunderstorm period. This results in 221*774 =171054 pairs with different response values. Based on the GPS lightning index, a pair is concordant if the *yes* lightning event has a higher probability by the sum of their individual estimated probabilities being greater than the observed lightning events, discordant if the opposite is true, and tied if the probabilities are equal. These values are used as a comparative measure of prediction. Measures of association (Table 5) show the number and percentage of concordant, discordant, and tied pairs. These values measure the association between the observed responses and the predicted probabilities.

a. Testing the GPS Lightning Index

The lightning index was tested on data from the thunderstorm season. In order obtain the proper predictand (index value), Wilks (1995), suggests using

$$\hat{y} = \frac{1}{1 + \exp(\beta_0 + \beta_1 x_1 + \beta_2 x_2 + \beta_3 x_3 + \beta_4 x_4)}, \qquad (4)$$

where $\hat{y}$ is the predictand (index value), β the coefficients for each predictor, **x** the value of the predictor, and the subscripts indicate which predictor it is for. In this case, using the GPS lightning index coefficients for each predictor, Eq. (5) becomes

$$\hat{y} = \frac{1}{1 + \exp(-6.7866 + .0011359x_1 + .06063x_2 + 0.32341x_3 + .06728x_4)} \qquad (5)$$

The meaning of this equation is most easily understood in the limits, as $(\beta_0 + \beta_1 x_1 + \beta_2 x_2 + \beta_3 x_3 + \beta_4 x_4) \rightarrow \pm \infty$. As the exponential function in the denominator becomes arbitrarily large, the predicted value approaches zero, indicating a lightning strike. As the exponential function in the denominator approaches zero, the index value approaches one, indicating a non-event. Thus, it is guaranteed that the logistic regression will produce properly bounded probability estimates. The index value was calculated for the entire data set for both test periods.

The index time series for each day during the thunderstorm period were reviewed to identify recurring patterns and the best index threshold value (ITV). Index values for non-event days typically fluctuate very close to 1.0 (Fig. 7). When index value falls below 0.7, lightning events follow. An ITV of 0.7 showed the best predictive skill was proved to be best suited for a forecast threshold. A level of 0.8 often recovered to 0.9, indicating a non-lightning event, while a level of 0.6 provided insufficient lead time before the first strike. A running mean time series of index values 10–12 hours prior to the first strike graphically captures the predictive value of the GPS lightning index. Figures 7c-e depict typical lightning event days. In these cases, the ITV was reached up to ten hours prior to the first strike.

b. Categorical Forecasts for the Thunderstorm Season

Forecast verification is needed to test the predictive accuracy of the GPS lightning index. Anytime the index value fell below the ITV and up to 90 minutes prior to first strike (meeting 90 minutes desired lead time), it was counted as a *yes* forecast. A contingency table (Table 6) is used to evaluate the GPS lightning index's prediction capabilities (Wilks 1995). For the thunderstorm period (subscript n), there were a total of 46 days evaluated. Twenty-five thunderstorms days were observed and forecast by the GPS lightning index (quadrant a). Five thunderstorms days were

forecast to occur but did not (quadrant b). Three storm days were observed to occur but the model failed to respond (quadrant c). In 13 remaining days the model did not forecast a lightning event and none was observed (quadrant d). The data from these quadrants are now used to determine the accuracy measures for a binary forecast. In particular the false alarm rate (FAR) is a measure of the forecast events that fail to materialize: FAR = b/(a+b). The probability of detection (POD) is a measure of the forecast events that did occur: POD = a/(a+c). The results of these calculations are shown in Table 7. The GPS lightning index proved its utility, particularly in the area of false alarm rates (FAR).

Although the thunderstorm season data are not statistically independent, the application of the GPS lightning index to these data reduced the FAR to 16.6%. This is a decrease of 26% of the KSC's previous FAR. The probability of detection (POD) result was only 8% less than the KSC POD for last season. In making these comparisons it should be noted that the time window of the GPS lightning index is 12.5 hours. The time window associated with KSC forecasts varies with synoptic situation, but is 4 to 6 hours on average.

c. Categorical Forecasts for the Independent Preseason

Using the same 90-minute desired lead time and ITV criteria for the independent preseason (subscript i, Table 6), there were a total of 21 days evaluated. Seven thunderstorms days were observed and forecast by the GPS lightning index (quadrant a). Three thunderstorm days were forecast to occur but did not (quadrant b). One storm day was observed to occur but the model failed to respond (quadrant c). In 10 remaining days the model did not forecast a lightning event and none was observed (quadrant d). The data from these quadrants are again used to determine the

accuracy measures for a binary forecast (FAR and POD). The results of these calculations are shown in Table 8.

GPS lightning index results for FAR in the independent preseason were 13.2% lower than KSC results of 43.2% (Table 8). POD was down by only 10%. These measures could easily be improved by adding forecaster's input of additional knowledge. Reference to satellite and Doppler radar data would give a forecaster the benefit of knowing the tracks and intensities of thunderstorms moving into the area. The GPS lightning index's capability to improve FARs would enhance mission readiness. Mission functions that cease for lightning would not be delayed by a forecast of lightning that does occur.

Results for the thunderstorm season are slightly better than for the preseason. This is attributed to seasonal availability in the moisture of the atmosphere during the summer season. The GPS trends show an increase in the amount of IPWV as well as more fluctuations during the thunderstorm season.

As with any attempt to forecast a meteorological event, timing is critical. The lightning model output indicates a potential when the ITV is met. To get a better understanding of how the GPS lightning index performs with regard to the timing of the first strike, the distribution of lead times once the ITV is met is plotted in Fig. 8a. A wide range of lead times (0-12 hours) is see, with an approximately normal distribution. The majority of the lead-times fall between 3 and 7.5 hours.

d. Missed Events

During the independent test the first missed event occurred on 19 May 1999 (Fig. 8b). The GPS lightning index forecast the lightning event, but on1y 1 hour prior to first strike, thus not meeting the 90-minute required lead time. An event on 13 May 1999 is a prime example of a false

alarm (Fig. 8c). Observations on this day show early morning fog that may have inhibited development of convection. However, the ITV was met and no lightning occurred.

The GPS lightning index was checked to see how it handled rain showers with no lightning, nocturnal events, and back to back events. Figure 8d depicts a day marked by distant nocturnal lightning (>30 nm from KSC)**,** morning fog, and afternoon towering cumulus in all quadrants. Although the index shows fluctuations, the ITV was never met, and the lightning index correctly handled this event. During a nocturnal example (Fig. 8e), the ITV was met seven hours prior to the first strike around midnight. Finally, the lightning index captured back-to-back events (Fig. 8f). In this case, a nocturnal thunderstorm ended just around midnight. Nine hours later the ITV was met and the first strike followed 4.5 hours later.

An interesting phenomena that occurs frequently in the time series after the ITV is met, is the tendency for a flatness or increase in the index prior to the first strike (e.g., Figs. 7e and f and Fig. 8e). This may be a reflection of compensating mesoscale subsidence associated with developing thunderstorms drying out the atmosphere above the GPS site.

5. Summary and Conclusions

A new GPS lightning index is developed to provide a tool for forecasting the Kennedy Space Center's primary weather challenge. A thunderstorm season (6/10/99 – 9/26/99) and a preseason (4/14/99 – 6/9/99) were chosen to develop and evaluate the GPS lightning index after examining a year's worth of operational GPS IPWV data with reference to the climatology of lightning occurrence in southern Florida. A binary logistic regression model was used to identify which of a set of 23 predictors contributed skill in forecasting a lightning event. Four predictors proved

important for forecasting lightning events; maximum electric field mill values, GPS IPWV, the 9-hour change (Δ9-hr) of IPWV, and K index.

Maximum electric field mill values increased substantially during inclement weather when the potential for lightning existed, sometimes reaching values of 12,000 V/m during a lightning event. But this variable lacked sufficiently long-term (90-minute plus) predictability. Composites of GPS IPWV and Δ9-hr IPWV several hours prior to an initial lightning strike show an increase of precipitable water for the site. By using current GPS-IPWV and Δ9-hr IPWV values, the model captures the current IPWV of the atmosphere but also changes in mid-level moisture associated with diurnal and synoptic scale circulations. The KI diagnoses convective activity by examining the moisture in the layer from 850 mb to 700 mb and the stability of the lapse rate. Given the fact that the three of the variables are sensitive to moisture, it important to note that they are not well correlated. The highest correlation coefficient was 0.47 between IPWV and KI.

The *GPS lightning index* is a binary logistic regression equation that includes the four predictors multiplied by their coefficients. When a time series of the GPS lightning index is plotted, a common pattern emerges. Whenever the lightning index drops to 0.7 or below, lightning follows within 12.5 hours. An index threshold value (ITV) of 0.7 was identified, and lightning events are forecast whenever the ITV is met. Forecast verification results obtained by using a contingency table revealed a 26.6% decrease from the Cape's previous season false alarm rates during the thunderstorm season, while obtaining a 13.2% decrease in false alarm rates for the preseason. For the KSC, a decreases in false alarm rates means that missions will not be halted for a forecast lightning event that does not occur. Additionally, the Cape met their desired lead time (90-minute notification) 79.1% of the time last year. Because the forecast verification was set up with reference to the 90-minute desired lead time criteria, POD results from the thunderstorm test

period (89.2%) and the preseason (87.5%) also reflect the desired lead time statistic. In this research, if a storm failed to meet the desired lead it was counted as a missed event. Thus, the GPS lightning index also improves the previous lead time at KSC by 10%.

The primary utility of the GPS lightning index is in alerting a forecaster to the possibility of lightning. Armed with the lightning index time series, a forecaster can improve the lead time and false alarm rate in lightning forecasts. However, the lightning index has a fairly large time window within which the lightning can occur. Therefore, the forecaster needs to rely on other resources such as radar and satellite to help refine the timing of the lightning event.

Future work will consist of testing the GPS lightning index using data from future thunderstorm seasons. It may be possible to refine the index with the addition of predictor variables not included in this study, such as low-level divergence, thunderstorm motion, radar data, instability indices, etc.

If the GPS lightning index fulfills its early promise, it may be useful to consider a similar statistical approach to help predict related weather phenomena. Observations show a correlation between increases of GPS IPWV and heavy precipitation (Businger et al. 1996), suggesting that a logistic regression model could provide the basis for a new flash-flood index.

6. Acknowledgments

The data resources and collection that went into this research were substantial and could not have been accomplished without special assistance from James Foster, Mike Bevis and Susan Derussy. We would like to thank Gary Barnes and Pao-Shin Chu for numerous suggestions for improvements in an early draft of the manuscript. Nancy Hulbirt provided assistance with the

figures. This research was supported by the U.S. Air Force through its Air Weather program and NOAA grant NA67RJ0154. This paper is SOEST contribution number xxxx.

7. References

Arritt, R. W., 1993: Effects of large-scale flow on characteristic features of the sea-breeze. *J. Appl. Meteor*., **32**, 116-125.

Bauman, W. H. and S. Businger, 1996: Nowcasting for Space Shuttle landings at Kennedy Space Center, Florida. *Bull. Amer. Meteor. Soc.*, **77**, 2295-2305.

_____, W. H., S. Businger, and M.L. Kaplan, 1997: Nowcasting Convective Activity for Space Shuttle Landings during Easterly Flow Regimes. *Wea. Forecasting*, **12**, 78-107.

Bevis, M., S. Businger, T. A. Herring, C. Rocken, S. R. A. Anthes, and R. H. Ware, 1992: GPS meteorology: Remote sensing of atmospheric water vapor using the Global Positioning System. *J. Geophys. Res.*, **97**, 15,787-15,801.

_____, S. Businger, S. Chiswell, T. A. Herring, R. A. Anthes, C. Rocken, and R. H. Ware, 1994: GPS meteorology: Mapping zenith wet delay onto precipitable water. *J. Appl. Meteor*., **33**, 379-386.

Blanchard, D. O., and R. E. Lopez, 1985: Spatial patterns of convection in south Florida. *Mon. Wea. Rev*.,**113**, 1282-1299.

Boybeyi, Z., and S. Raman, 1992: A three-dimensional numerical sensitivity study of convection over the Florida peninsula. *Bound.-Layer Meteor.*, **60**, 325-359.

Businger, S., M. Bevis, S. Chiswell, M. Bevis, J. Duan, R. Anthes, and R. Ware, C. Rocken, M. Exner, T. VanHove, and F. Solheim, 1996: The Promise of GPS in atmospheric monitoring. *Bull. Amer. Meteor. Soc.*, **77**, 5-17.

Duan, J., S. Businger, M. Bevis, S. Chiswell, M. Bevis, J. Duan, R. Ware, C. Rocken, P. Fang, Y. Bock, T. VanHove, F. Solheim S. McClusky, T. Herring, and R. King, 1996: GPS Meteorology: Direct estimation of the absolute value of perceptible water. *J. Appl. Meteor.*, **35**, 830-838.

Estoque, M. A.,1962: The sea breeze as a function of the prevailing synoptic situation. *J. Atmos. Sci.*, **19**, 24-25.

Fleagle, R. G., and J. A. Businger, 1980: *An Introduction to Atmospherics Physics.* Academic Press, New York. pp 432.

Foote, G. B., 1991: Scientific overview and operations plan for the convection and precipitation/ electrification program. National Center for Atmospheric Research, Boulder, CO, 145 pp.

Harms, D., B. Boyd, Rlucci, M Hinson, and M Maier, 1997: Systems used to evaluate the natural and triggered lightning threat to the eastern range and Kennedy Space Center. *28th Conference on Radar Meteorology*, 240-241

Hazen, D. S., W. P. Roeder, B. F. Lorens, and T. L. Wilde, 1995: Weather impacts on launch operations at the Eastern Range and Kennedy Space Center. Preprints, *Sixth Conf. On Aviation Weather Syatems*, Dallas, TX, Amer. Meteor. Soc., 270-275.

Hosmer, D. W., and S. Lemeshow, 1989: *Applied Logistic Regression*. Wiley, New York, 307 pp.

Marshall, T. C., W. D. Rust, M. Stolzenburg, W.P. Roeder,and P. R. Krehbiel, 1999: A study of enhanced fair-weather electric field occurring soon after sunrise. *J. Geophys. Res.*, **104,** 24455-24469.

Neumann, C. J., 1971: The thunderstorm forecasting system at the Kennedy Space Center. *J. Appl. Meteor*., **10**, 921-936.

Panofsky, H. A., and G. W. Brier, 1958: *Some Applications of Statistics to Meteorology*. University Park, Pennsylvania, 224 pp.

Pielke, R., 1974: A three-dimensional numerical model of the sea-breeze over south Florida. *Mon. Wea, Rev*., **102**, 115-139.

Reap, R. M., 1994: Analysis and prediction of lightning strike distributions associated with synoptic map types over Florida. *Mon. Wea. Rev.*, **122**, 1698-1715.

Watson, A. I., R.L. Holle, R. E. Lopez, R. Ortiz, and J. R. Nicholson, 1991: Surface convergence as a short term predictor of cloud-to-ground lightning at Kennedy Space Center. *Wea. Forecasting*, **6**, 49-64.

Wilks, D., 1995: *Statistical Methods in Atmospheric Sciences*. Academic Press, 464 pp.

Wolfe, D.E. and S.I. Gutman, 2000. Development of the NOAA/ERL Ground-Based GPS Water Vapor Demonstration Network: Design and Initial Results, *J. Atmos. Ocean. Technol,* 17, 426-440.

List of Figures

Fig. 8 (a) Time in hours prior to first-strike that LTV was met for all thunderstorms. Time series of GPS lightning index for (b) a lightning event in which the desired lead time was not met on 19 May 1999, (c) a false alarm event on 13 May 1999, (d) a day with no lightning event on 20 May 1999, (e) a nocturnal lightning event on 21-22 July 1999, and (f) back to back lightning events on 9 August 1999.

Table 1 Initial Predictors

Predictors	**Source of data**
1. GPS IPWV	GPS Sensor
2-13. ΔIPWV* from 1 to 12 hours	GPS Sensor
14. 30 min Field Mill Averages	Electric Field Mill
15. 30 min Field Mill Maximums	Electric Field Mill
16. Temperature	GPS Sensor
17. Pressure	GPS Sensor
18. Dewpoint Temperature	Surface Observation
19. Total Totals	RAOB
20. Freezing Level	RAOB
21. Wind Direction	Surface Observation
22. K Index	RAOB
23. 700 mb Vertical Velocity	ETA Model

* Δ means change

Table 2 Logistic Regression Table

Predictor	Coefficient	Standard Deviation	Z-Value	p-Value	Odds Ratio
Constant	-6.7866	0.7208	-9.42	0.000	
Max V/m	0.0011359	0.0002923	3.89	0.000	1.00
IPWV	0.06063	0.01467	4.13	0.000	1.06
Δ9 IPWV	0.32341	0.02961	10.92	0.000	1.38
K-Index	0.06728	0.02081	3.23	0.001	1.07

Table 3 Goodness of Fit Tests

Method	p-Value
Pearson Residual	1.000
Deviance Residual	1.000
Hosmer-Lemeshow	.605

Table 4 Observed and Expected Frequencies

	Group										
Value	1	2	3	4	5	6	7	8	9	10	Total
Yes											
Obs	0	0	2	6	16	15	26	38	42	76	221
Exp	.3	1.1	2.7	6.2	11.2	17.5	25.8	35.2	47.6	73.3	
No											
Obs	99	100	97	94	83	85	73	62	57	24	774
Exp	98.7	98.9	96.3	93.8	87.8	82.5	73.2	64.8	51.4	26.7	
Total	99	100	99	100	99	100	99	100	99	100	995

Table 5 Measures of Association

Pairs	Number	Percent
Concordant	146424	85.6%
Discordant	24299	14.2%
Ties	331	.2%
Total	171054	100%

Table 6 Contingency Table for Categorical Forecast of Discrete Predictands.

	Observed Yes	No
Model Forecast Yes	$a_n = 25$ $a_i = 7$	$b_n = 5$ $b_i = 3$
No	$c_n = 3$ $c_i = 1$	$d_n = 13$ $d_i = 10$

Relationship between counts (letters a-d) of forecast event pairs for the dichotomous categorical verification. Quadrant *a* denotes the occasions when the lightning was forecast to occur and did. Quadrant *b* denotes the occasions when the lightning was forecast to occur but did not. Quadrant *c* denotes the occasions when the lightning was not forecast to occur but did. Quadrant *d* denotes the occasions when the lightning was not forecast to occur and did not. Subscripts n and i indicate non-independent test (thunderstorm period) and independent test (preseason).

Table 7 Thunderstorm Season Test Results (10 June to 26 September 1999).

	GPS Lightning Results	KSC Results From 1999 Season
False Alarm Rate:	16.6%	43.2%
Hit Rate:	82.6%	N/A
Threat Score:	75.6%	N/A
Probability of Detection:	89.2%	97.5%

Table 8 Independent Test Results (Preseason, 14 April to 9 June 1999).

	GPS Lightning Results	KSC Results From 1999 Season
False Alarm Rate:	30%	43.2%
Hit Rate:	80.9%	N/A
Threat Score:	63.6%	N/A
Probability of Detection:	87.5%	97.5%

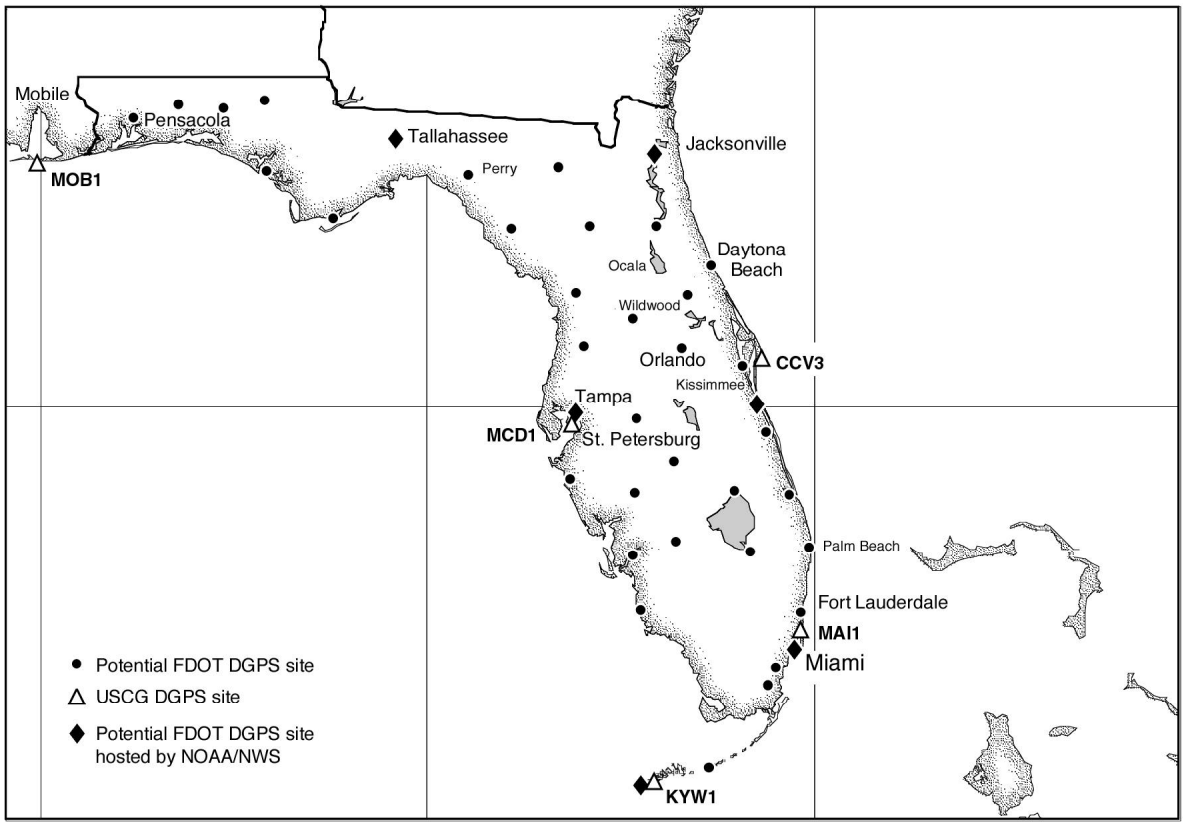

Fig. 1 Current and planned GPS Sites in Florida.

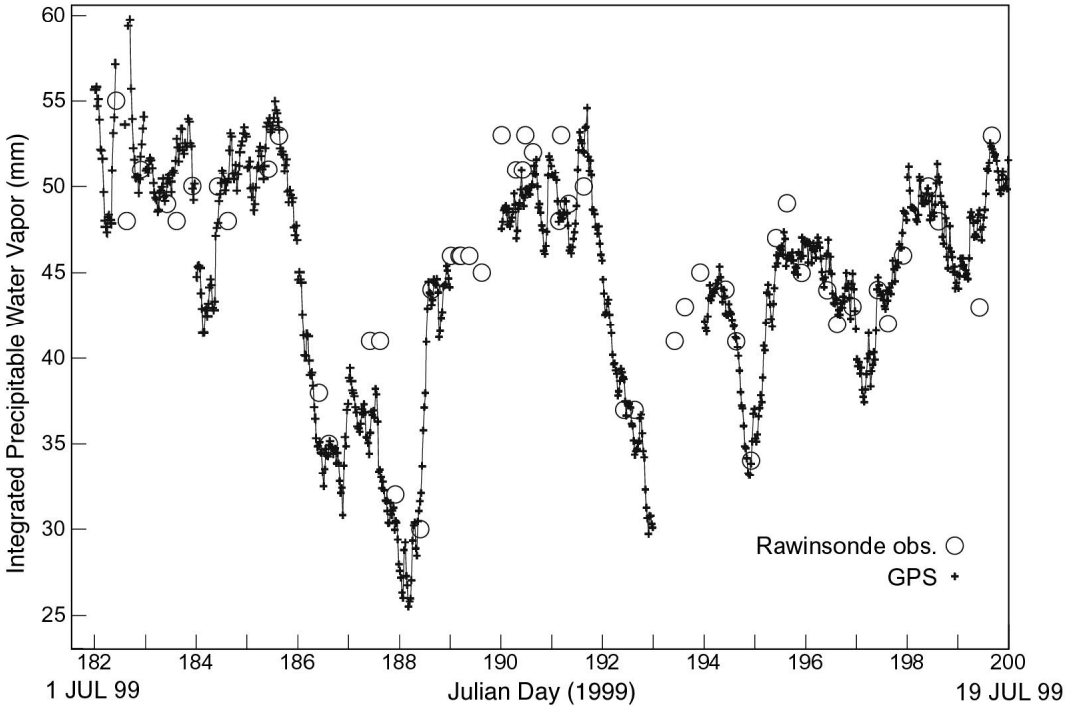

Fig. 2 Comparison of column integrated water vapor from rawinsondes launched by the 45th Weather Squadron at Patrick AFB, Florida (circles) with GPS observations made at the U.S. Coast Guard Differential GPS site (CCV3) at Cape Canaveral, Florida. Rawinsonde data courtesy of Susan Derussy.

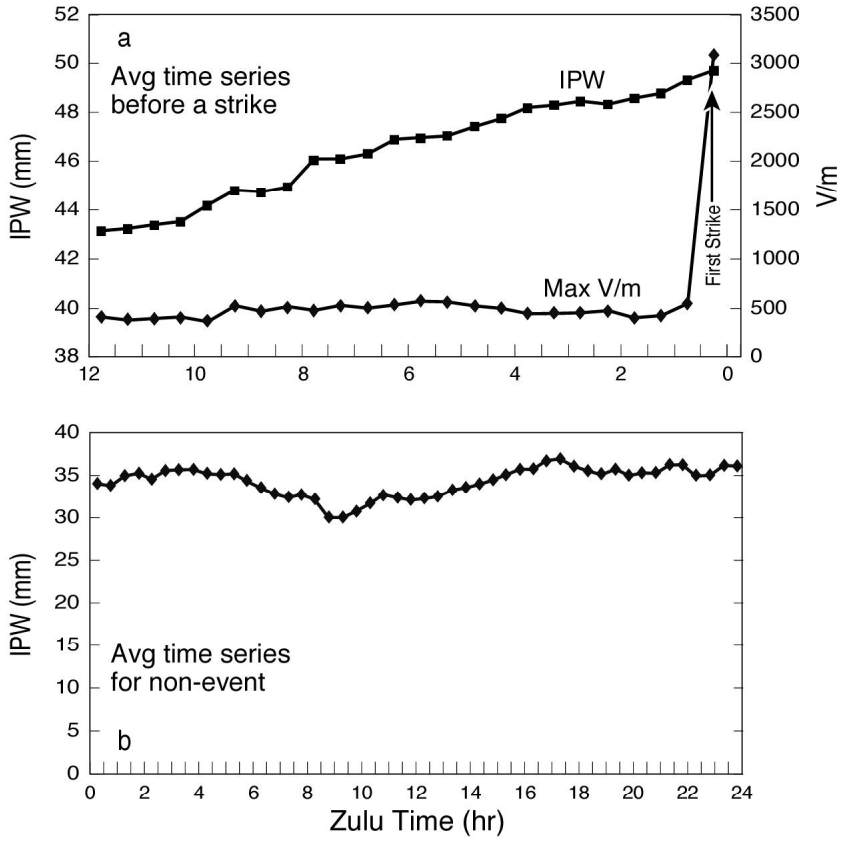

Fig. 3 (a) Average time series of GPS IPWV and maximum electric field mills values for the hours leading up to a lightning strike. (b) GPS IPWV 24-hour average time series for non-event weather days.

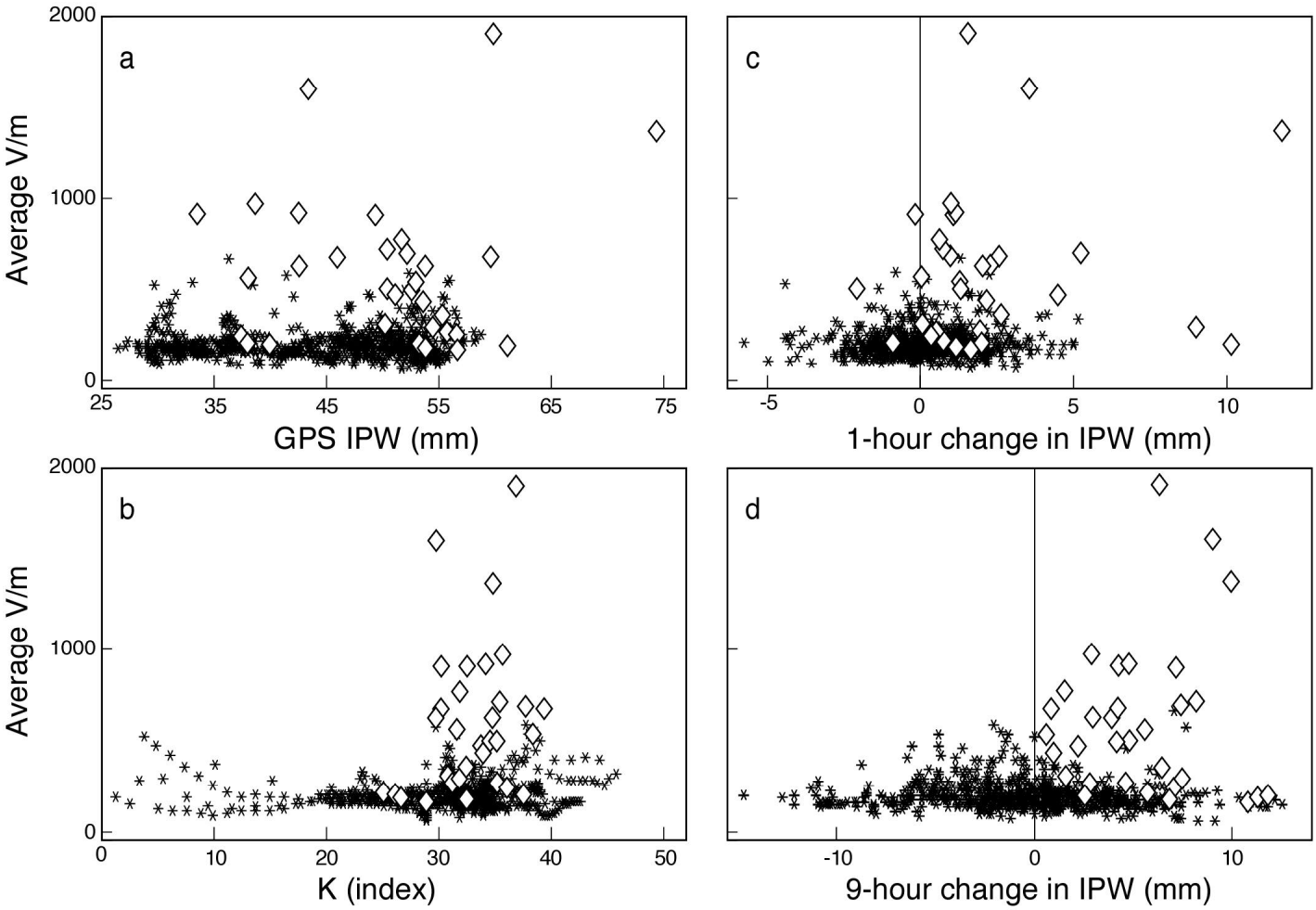

Fig. 4 (a) Scatter plot of average electric field mill values and GPS IPWV. (b) Scatter plot of average electric field mill values and K index. (c) Scatter plot of average electric field mill values and ∆1-hr GPS IPWV. (d) Scatter plot of average electric field mill values and ∆9-hr GPS IPWV. White diamonds denote lightning detected, black asterisks denote no lightning detected.

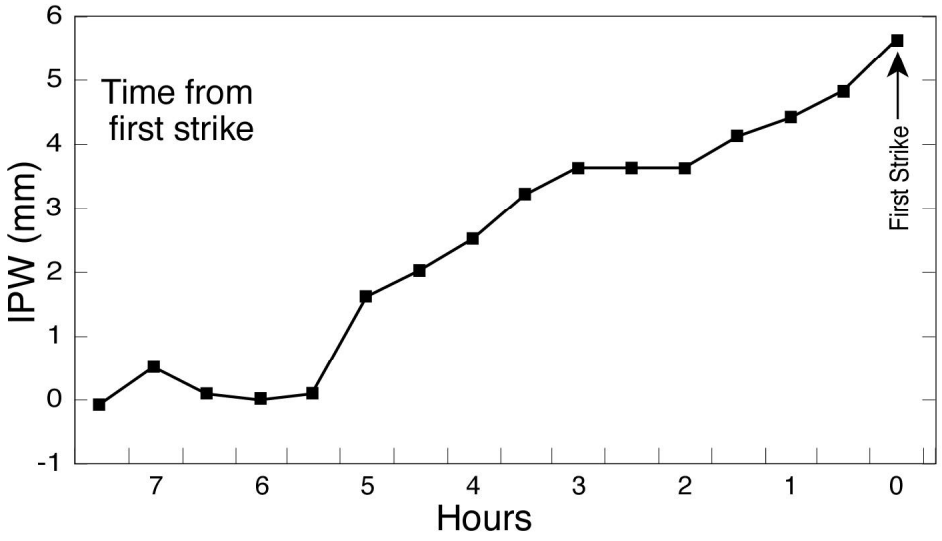

Fig. 5 Composite time series of the average change in Δ 9-hr GPS IPWV from one hour to the next, using the superposed epoch method with the time of the first strike defined as the zero hour.

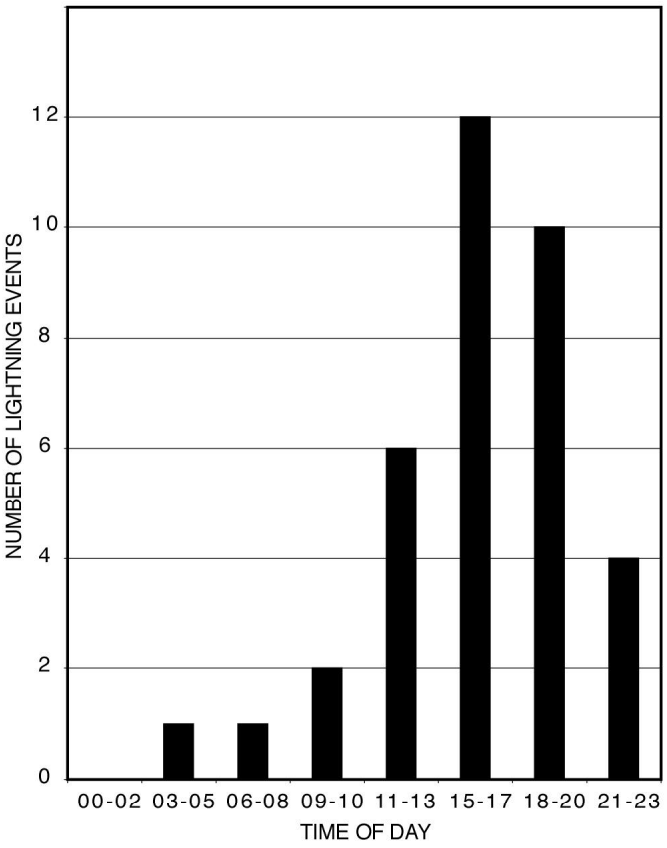

Fig. 6 Histogram of time of day of lightning occurrence at Cape Canaveral. Histogram includes data from both test periods.

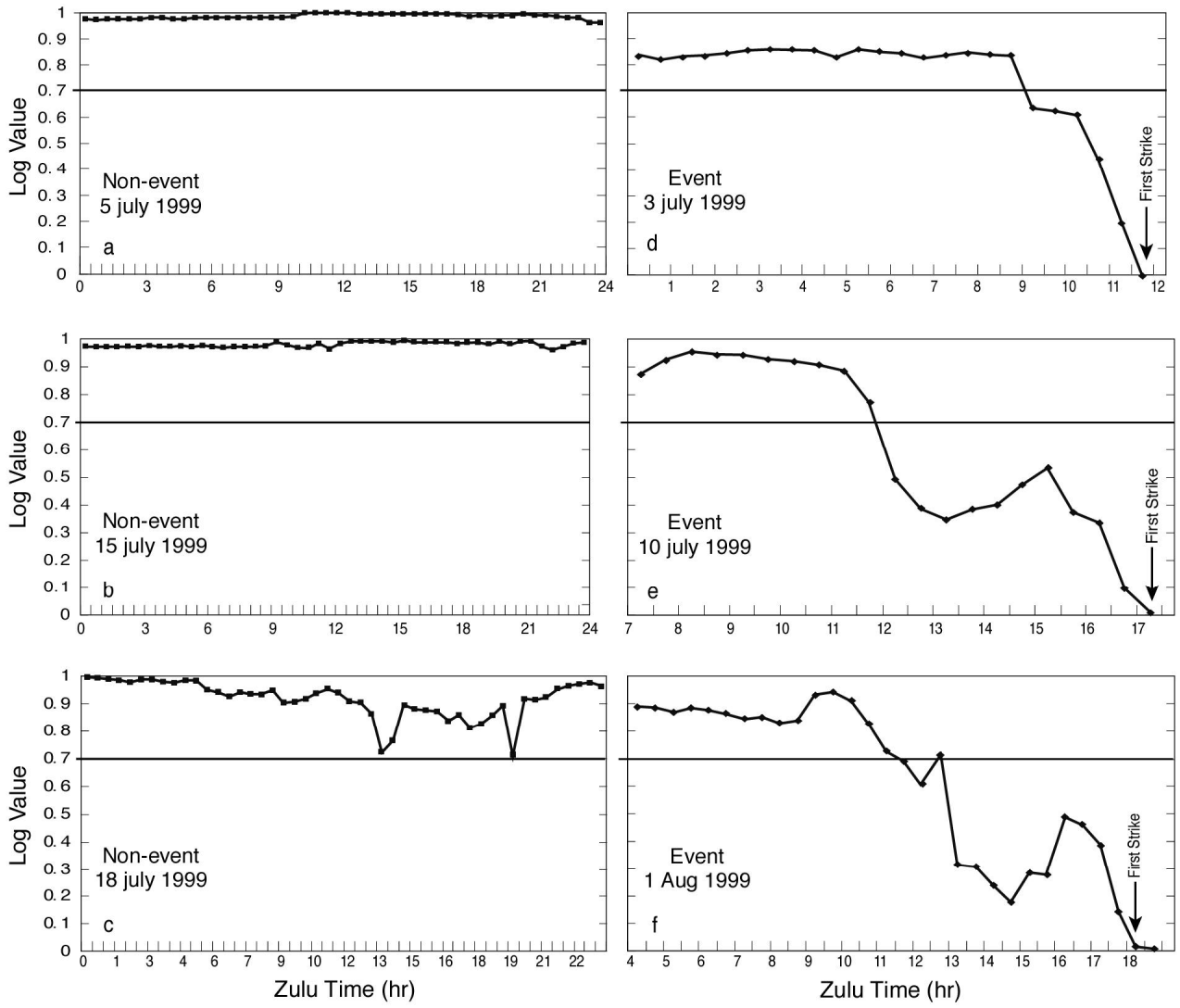

Fig. 7 Time series of GPS lightning index for (a) a non-event day, 5 July 1999, (b) a non-event day, 15 July 1999, (c) a non-event day, 18 July 1999, (d) a lightning event on 3 July 1999, (e) a lightning event on 10 Jul 1999, and (f) a lightning event on 1 August 1999.

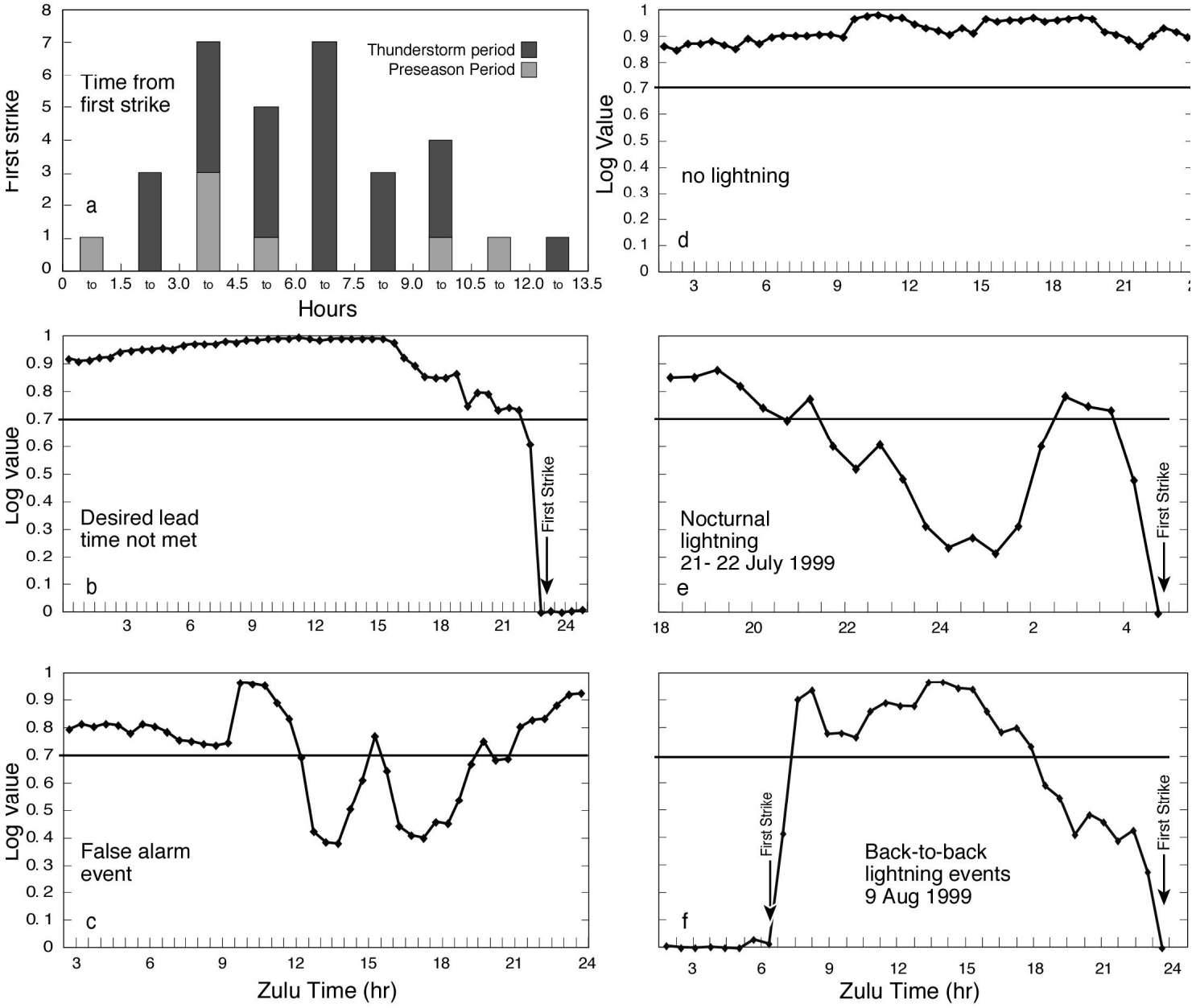

Fig. 8 (a) Time in hours prior to first-strike that LTV was met for all thunderstorms. Time series of GPS lightning index for (b) a lightning event in which the desired lead time was not met on 19 May 1999, (c) a false alarm event on 13 May 1999, (d) a day with no lightning event on 20 May 1999, (e) a nocturnal lightning event on 21-22 July 1999, and (f) back to back lightning events on 9 August 1999.